FUGITIVE GAS EMISSION RATE ESTIMATION USING MULTIPLE HETEROGENEOUS MOBILE SENSORS

Jake R. Gemerek
Mechanical and Aerospace Engineering,
Cornell University

Silvia Ferrari
Mechanical and Aerospace Engineering,
Cornell University

John D. Albertson
Civil and Environmental Engineering,
Cornell University

***Abstract*—This paper presents an approach for autonomous and reliable localization of fugitive methane emissions and quantification of source emission rates over large regions of interest. Previous methods have used single mobile unmanned ground vehicle (UGV) leak localization, but as a result cannot disambiguate multiple sources when plumes overlap. The novel method presented in this paper implements a mobile heterogeneous sensor network comprised of aerial- and ground-based platforms equipped with on-board concentration sensors. The UGVs use a recursive Bayesian method to probabilistically determine all source rates in a region of interest (RoI). Using a flux estimation method for path integrated concentration measurements surrounding a point source, unmanned aerial vehicles (UAVs) are shown to reliably estimate source emission rates. By communicating information about concentration measurements to the UAVs, the UGVs are shown able to collaboratively plan efficient measurement paths resulting in accurate disambiguation and estimation of all source emission rates in the RoI.**

***Index Terms*—Fugitive Emissions, Mobile Sensor Networks, Heterogeneous Sensor Networks.**

1. INTRODUCTION AND PROBLEM FORMULATION

Natural gas is considered to be one of the most beneficial fossil fuels, that may help meet the need for reduced greenhouse gas emissions and the desire to become less dependent on imported petroleum resources. Also, domestic energy production is favored by natural gas since there are large reserves within North America [1], and accessible reserves are significantly larger now due to recent advances in drilling technology [2]. Because natural gas is composed primarily of methane, system leaks lead to increased global warming potential, making natural gas less attractive when compared to other fossil fuels [3]. In order for natural gas to be a sustainable resource for future decades, rapid leak detection systems are needed to help reduce overall methane emissions.

This paper demonstrates that the use of a heterogeneous mobile sensor network comprised of UGVs and UAVs equipped with point-concentration sensors, and path-integrated concentration sensors, respectively, can estimate source emission rates more reliably than a homogeneous sensor network in the presence of multiple sources characterized by plumes that are potentially overlapping. Overlapping plume footprints, or volumes where a concentration measurement would be expected based on meteorological conditions, lead to difficulty in determining which upwind source is responsible for a single concentration measurement. A network of heterogeneous, mobile sensors with complimentary capabilities can intelligently plan their measurement trajectories such that individual source emission rates are estimated with high confidence even with multiple overlapping plume footprints.

This paper considers the problem of estimating the emission rates of multiple sources in a region of interest (RoI) using an inexpensive ground-based point-concentration sensor in collaboration with an air-based laser. The ground-based sensor consists of an UGV equipped with an on-board methane point concentration sensor and with autonomous computing and wireless communication capabilities, which performs measurements along known roadways to provide an initial probabilistic source emission rate for all sources in the RoI. The air-based sensor consists of an UAV equipped with a laser that provides methane path-integrated concentrations processed by on-board computing and used to disambiguate source contributions with overlapping footprints.

Consider the RoI $\mathcal{W} \subset \mathbb{R}^3$ populated by N point emission sources $\mathcal{T}_1, ..., \mathcal{T}_N$ labeled by the index set L_T. Every potential source $\mathcal{T}_l$, where $l \in L_T$, is located at a known position vector $\mathbf{x}_l \in \mathbb{R}^3$ and has scalar source emission rate $S_l \in \mathbb{R}$. Let $\mathbf{x}_l$ be defined with respect to a fixed Cartesian frame $\mathcal{F}_\mathcal{W} \in \mathcal{W}$, with origin $\mathcal{O}_\mathcal{W}$, and let $\mathcal{F}_{\mathcal{T}_l} \in \mathcal{W}$ denote a fixed Cartesian frame with origin $\mathcal{O}_{\mathcal{T}_l}$ at $\mathbf{x}_l$ (figure 1). Each source is assigned a seperate reference frame because the model used to calculate a sources contribution to the net concentration at a point is a function of the lateral (η) and downwind (ξ) position relative to the source position. The frame $\mathcal{F}_{\mathcal{T}_l}$ is rotated by an angle θ_w relative to $\mathcal{F}_\mathcal{W}$ such that it is aligned with the average wind velocity $\mathbf{u} \in \mathbb{R}^3$, as shown in figure 1. The transformation from the source-fixed frame $\mathcal{F}_{\mathcal{T}_l}$ to $\mathcal{F}_\mathcal{W}$ is performed using the rotation matrix

$$\mathbf{R} = \begin{bmatrix} \cos\theta_w & \sin\theta_w & 0 \\ -\sin\theta_w & \cos\theta_w & 0 \\ 0 & 0 & 1 \end{bmatrix} \tag{1}$$

The UGV is assumed to be a road vehicle that is constrained to travel on known roadways in the RoI, $\mathcal{W}$, denoted by $\mathcal{H} \subset \mathcal{W}$. The UGV path $\mathcal{Q} \subset \mathcal{H}$ is the set of all UGV positions $\mathbf{q} \in \mathcal{Q}$ defined with respect to $\mathcal{F}_\mathcal{W}$. $\mathcal{Q}$ is chosen such that as many useful measurements as possible are taken, given roadway constraints. The UAV path $\mathcal{R}$ is constrained such that it flies at a constant height for the entire path, and it can only fly a total distance d. The UAVs position $\mathbf{r} \in \mathcal{R}$ is defined with respect to $\mathcal{F}_\mathcal{W}$. The problem considered in this paper is to use the information, regarding all sources within a RoI, collected by the UGV to plan a short path for the UAV to collect information about select sources that proves useful to the overall objective of accurately estimating all source emission rates.

2. PLUME MODELING

The model used in this paper for calculating the time-averaged concentration field has been proven useful for mobile sensing applicationsin in previous work [4] . The methane concentration of interest is defined as the difference from background ambient

978-1-5090-2392-9/17/$31.00 ©2017 IEEE

concentration, which is about 1.8 ppm. This model is also used to simulate sensor measurements, as explained in the following section. Simulation of instantaneous measurements using a time-averaged concentration is performed by introducing a random variable which accounts for both model inaccuracies and sensor noise.

Consider an arbitrary point $P \in \mathcal{W}$, with a position described by the vector $\mathbf{p} = \begin{bmatrix} \xi & \eta & z \end{bmatrix}^T$, defined relative to $\mathcal{F}_{\mathcal{T}_l}$. The time-averaged concentration at P caused by source $\mathcal{T}_l$ with source rate S_l is,

$$C_l(\mathbf{p}) = \frac{S_l}{\bar{U}} D_\eta(\xi, \eta) D_z(\xi, z) \tag{2}$$

where $\bar{U}$ is the effective speed of plume advection, and $D_\eta(\xi, \eta)$ and $D_z(\xi, z)$ account for the lateral and vertical dispersion of the plume, respectively. The lateral dispersion $D_\eta(\xi, \eta)$ is commonly assumed to be Gaussian with standard deviation related to wind fluctuations. The vertical dispersion is modeled by,

$$D_z(\xi, z) = \frac{A}{\bar{z}(\xi)} exp\left\{-\left(\frac{Bz}{\bar{z}(\xi)}\right)^s\right\} \tag{3}$$

where $\bar{z}(\xi)$ is the average plume height at ξ, while A, s, and B, are functions of atmospheric stability [5].

3. EMISSION RATE ESTIMATION

Two sensors are used in the proposed mobile network whose measurements are used to calculate probabilistic source emission rates; point concentration sensors mounted to UGV(s), and path-integrated laser concentration sensors mounted to UAV(s). In order to quantify the effectiveness of the proposed method, the sensing capabilities must be modeled to simulate real-world performance in the field, and also account for errors in the models used to calculate expected concentrations.

3.1. UGV

The UGV uses a point concentration methane sensor to measure the instantaneous concentration at the UGVs position $\mathbf{q}$. This measurement is simulated by summing the calculated time-averaged concentrations from each source and adding a random variable n, which follows a Gaussian distribution with zero mean, and standard deviation σ_n to simulate sensor noise and model errors. The simulated point-concentration measurement $\tilde{C}(\mathbf{q}, \sigma_n)$ is given by

$$\tilde{C}(\mathbf{q}, \sigma_n) = \sum_{l=1}^{N} C_l(\mathbf{q}) + n(\sigma_n) \tag{4}$$

This measurement is used to estimate the source emission rate of the lth source using Bayes' theorem. The probability of source emission rate S_l, given the current measurement set $\mathcal{M}$, RoI information $\mathcal{W}$, and meteorological conditions Λ, is given by

$$p(S_l|\mathcal{M}, \mathcal{W}, \Lambda) = \frac{p(S_l)p(\mathcal{M}|S_l, \mathcal{W}, \Lambda)}{\int_{\mathcal{M}} p(S_l)p(\mathcal{M} = m|S_l, \mathcal{W}, \Lambda)dm} \tag{5}$$

Before the measurements are taken, there is no prior source emission rate information $p(S_l)$, so it is initialized as a uniform distribution. The Gaussian likelihood function

$$p(\mathcal{M}|S_l, \mathcal{W}, \Lambda) = \frac{1}{\sigma_e\sqrt{2\pi}} exp\left[-\frac{1}{2}\left(\frac{m - C_l(\mathbf{q})}{\sigma_e}\right)^2\right] \tag{6}$$

represents the probability of a measurement set $\mathcal{M}$, assuming a hypothetical S_l. Once a measurement is obtained at a location $\mathbf{q}$, and the posterior probabilistic source emission rate $p(S_l|\mathcal{M}, \mathcal{W}, \Lambda)$ is calculated for each source, the prior distribution for each source is updated to the posterior distribution for the most recent measurement.

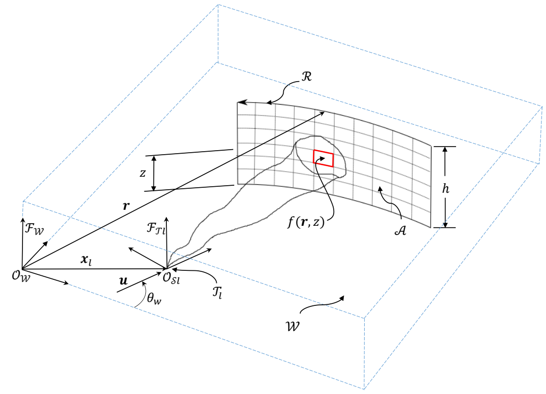

Figure 1. Diagram of Cartesian reference frames, where $\mathcal{F}_{\mathcal{W}}$ is an inertial frame and $\mathcal{F}_{\mathcal{S}_l}$ is a fixed frame at source location $\mathbf{x}_l$ and rotated an angle θ_w with respect to $\mathcal{F}_{\mathcal{W}}$. Also, the flux of fugitive gas across a point on the imaginary surface $\mathcal{A}$ defined by the aerial vehicle's path $\mathcal{R}$ and height h.

3.2. UAV

The UAVs measure the path integrated concentration in the vertical direction from the ground ($z = 0$) to the sensor's height ($z = h$) through laser reflections. These measurements are used to estimate the mass flow rate $\dot{m}$ of fugitive gas across an imaginary vertical surface $\mathcal{A}$, defined by the UAV path $\mathcal{R}$, as shown in figure 1. The advective flux $f(\mathbf{r}, z)$ of fugitive gas across a point $a \in \mathcal{A}$ is the product of the concentration and air flow velocity component perpendicular to $\mathcal{A}$,

$$f(\mathbf{r}, z) = C(\mathbf{r}, z)\mathbf{u}(z) \cdot \hat{\mathbf{n}}(\mathbf{r}) \tag{7}$$

where $\hat{\mathbf{n}}(\mathbf{r})$ is the outward unit vector normal to the surface $\mathcal{A}$. Since the flux will only be non-zero in the plume and the vertical length scale of the plume is small compared to the length scale for vertical variations in wind speed, the wind velocity $\mathbf{u}(z)$ can be approximated as constant and equal to the velocity at the average plume height $\bar{z}(\xi)$. The mass flow rate $\dot{m}$ across the surface $\mathcal{A}$ can now be calculated in terms of measurable quantities by integrating the flux over $\mathcal{A}$, which results in equation 8.

$$\dot{m} = \int_{\mathcal{R}} \tilde{C}^z(\mathbf{r})\mathbf{u}(\mathbf{r}) \cdot \hat{\mathbf{n}}(\mathbf{r})d\mathbf{r} \tag{8}$$

where $\tilde{C}^z(\mathbf{r})$ is the measured depth integrated concentration based on sensor precision and modeling errors.

$$\tilde{C}^z(\mathbf{r}) = \sum_{l=1}^{N} C_l^z(\mathbf{r}) + n(\sigma_n) \tag{9}$$

If the surface $\mathcal{A}$ is chosen to enclose a single source and the vehicle flies sufficiently high such that negligible gas escapes from above, then the mass flow rate of fugitive gas across the surface surrounding the source $\mathcal{T}_l$ can be used to estimate the source emission rate of that source S_l. From these measurements, the probabilistic source rate, $p(S_l|\mathcal{M}, \mathcal{W}, \Lambda)$, is modeled as a normal distribution with a mean value equal to the mass flow rate through a surface surrounding $\mathcal{T}_l$, and a standard deviation accounting for both model and sensor errors.

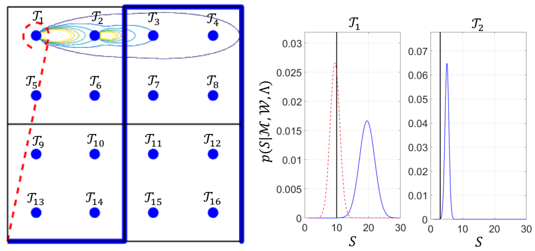

Figure 2. All sources, indicated as blue circles, have zero emission rate, except $S_1 = 10$ and $S_2 = 3$. All sensors are initially at the lower left intersection. The UGV and UAV paths (left) and resulting probabilistic emission rate estimates (right) are indicated as solid blue curves and dashed red curves, respectively

4. SIMULATION RESULTS

The simple RoI $\mathcal{W}$ used in this section (Figure 2) has been chosen for the purposes of demonstration, but the methods can be readily applied to a larger RoI. Figure 2 is generated from a simulation in which two sources ($\mathcal{T}_1$ and $\mathcal{T}_2$) leak and are characterized by an overlapping footprint. In this case, both source emission rates (S_1 and S_2) are overestimated by the ground vehicle (as shown in Figure 2). These results demonstrate that the UGV estimation is prone to significant error when there are overlapping plume footprints. For this reason, an UAV is needed to determine which upwind source is responsible for the high concentration measurements reported by the UGV.

The effectiveness of the UAV in diambiguating overlapping plumes is illustrated in Figure 2, where the UAV path corrects the inaccurate prediction of the emission rate based on the UGV data. Since the UAV is constrained by its battery life, the UAV path is chosen to only obtain an estimate of S_1 because the mean probabilistic source emission rate predicted by the UGV is above a predefined threshold (10 in this simulation). In this method, the sources to be visited by the UAV are chosen by ranking their mean emission rate estimate and determining if this mean is above a specified actionable threshold. Then, the UAV path is chosen by connecting the current UAV position to the closest source with a mean above this threshold. The resulting path and probabilistic emission rates for all sources are shown in Figures 3 and 4. The simulation results are obtained using an arbitrary wind angle and actual source emission rates. The resulting probabilistic emission rates in Figure 4 show that the mean estimate for all sources provides an accurate prediction of the actual emission rate once the UAV completes its measurement path based on the feedback provided by the UGV.

5. CONCLUSION

A novel hierarchical approach for robustly localizing and characterizing fugitive methane leaks is presented to provide a means for drastic mitigation of environmental impact from natural gas production. With the ability to autonomously and reliably localize fugitive emissions, sources found to be leaking above a prescribed threshold may be mitigated quickly after leak detection. The use of heterogeneous vehicles has proven to determine source emission rates more confidently by leveraging the strengths and weaknesses of the different mobile sensing platforms. Simulation results obtained for one UGV constrained to drive along roadways has proven to lead to incorrect estimation of source emission rates when plume footprints overlap. However, when used to guide an UAV to obtain additional path-integrated measurements, the leaks are localized reliably and their emission rates estimated accurately. Given the advancement of this robust source rate estimation method, future work will focus on optimal path planning and communication for heterogeneous mobile sensor networks with realistic constraints on the mobile platforms and experimental validation.

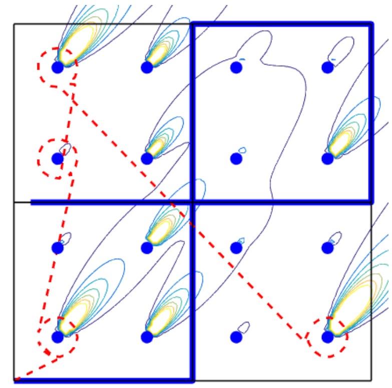

Figure 3. Arbitrary wind angle and source emission rates for all sources with the ground vehicle path indicated as the blue line, and the UAV path indicated by the dashed red line.

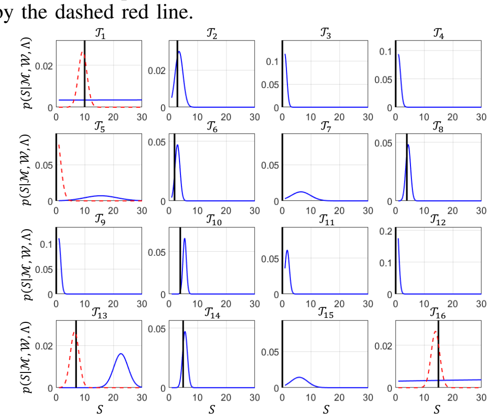

Figure 4. Probabilistic source emission rates. The blue curves are generated from the UGV data and the red dashed curves are generated from the UAV data. The vertical black lines are the actual emission rate.

References

[1] (2015) Natural gas annual report. U.S. Energy Information Administration. [Online]. Available: http://www.eia.gov/naturalgas/annual/pdf/nga15.pdf

[2] Q. Wanga, X. Chena, A. N. Jhac, and H. Rogersd, "Natural gas form shale formation - the evolution, evidences and challenges of shale gas revolution in united states," *Renewable Sustainable Energy Rev*, vol. 30, pp. 1–28, 2014.

[3] A. R. Brandt, G. A. Heath, E. A. Kort, F. O'Sullivan, G. Ptron, S. M. Jordaan, P. Tans, J. Wilcox, A. M. Gopstein, D. Arent, S. Wofsy, N. J. Brown, R. Bradley, G. D. Stucky, D. Eardley, and R. Harriss, "Methane leaks from north american natural gas systems," *Energy and Environment*, vol. 343, pp. 733–735, 02 2014.

[4] J. Albertson, T. Harvey, G. Foderaro, ingping Zhu, X. Zhou, S. F. M. S. Amin, M. Modrak, H. Brantley, and E. D. Thoma, "A mobile sensing approach for regional surveillance of fugitive methane emissions in oil and gas production," *Environmental Science and Technology*, vol. 50, pp. 2487–2497, 2016.

[5] T. A. Foster-Wittig, E. D. Thoma, and J. D. Albertson, "Estimation of point source fugitive emission rates from a single sensor time series: A conditionally-sampled gaussian plume reconstruction," *Atmospheric Environment*, vol. 115, pp. 101–109, 2015.